

D16
N79-20046

16

A STUDY OF THE INTERACTION OF A NORMAL SHOCK WAVE
WITH A TURBULENT BOUNDARY LAYER AT TRANSONIC SPEEDS*

A.F. Messiter and T.C. Adamson, Jr.
The University of Michigan

SUMMARY

An asymptotic description is derived for the interaction of a weak normal shock wave and a turbulent boundary layer along a plane wall. In the case studied the nondimensional friction velocity is small in comparison with the nondimensional shock strength, and the shock wave extends well into the boundary layer. Analytical results are described for the local pressure distribution and wall shear, and a criterion for incipient separation is proposed. A comparison of predicted pressures with available experimental data includes the effect of longitudinal wall curvature.

INTRODUCTION

In transonic flows a transition from supersonic to subsonic speeds typically occurs through a shock wave which is normal to a solid boundary. Across the boundary layer along this surface, the upstream fluid velocity decreases from its value in the external flow to zero at the wall, and the strength of an incident shock wave must decrease to zero in the supersonic part of the boundary layer; at the wall there is no discontinuity in pressure.

In the undisturbed turbulent boundary layer, viscous forces are important only in a very thin wall layer having thickness of the order of the local viscous length and velocity of the order of the friction velocity. In most of the boundary layer the mean velocity profile is nearly uniform, with a decrease from the external-flow value of the same order as the friction velocity. The flow changes caused by a weak incident normal shock wave will depend on the relative sizes of this velocity variation and the difference between the external-flow Mach number and one, i.e., on the ratio of the nondimensional friction velocity to the nondimensional shock-wave strength. Asymptotic flow descriptions have been derived for large (ref. 1), moderate (refs. 2,3,4) and small (ref. 5) values of this ratio, and the oblique-shock problem has also been studied (ref. 6). In each case the local mean pressure gradient and fluid deceleration are large enough that the flow near the shock wave may be described as an inviscid rotational flow in most of the boundary layer. In a thinner sublayer, changes in the turbulent stresses do influence the changes in velocity, and here some model must be chosen (e.g., a mixing-length model) for describing these stresses. The displacement effect of the flow changes in this sublayer is small enough that the dominant terms in the pressure are not affected. Thus the pressure is cal-

*This work was supported by NASA Langley Research Center, under Research Grant NSG 1326.

culated from the inviscid-flow equations and then is substituted into the sub-layer equations for the calculation of changes in wall shear.

The present work is a continuation of the work of reference 5. Asymptotic solutions are obtained in the limit as the nondimensional friction velocity and shock-wave strength approach zero, such that the ratio of friction velocity to shock strength also approaches zero, as does the distance from the wall to the undisturbed sonic line divided by the boundary-layer thickness. The pressures found in reference 5 are shown to be modified by higher-order and curvature effects, and the calculation of wall shear is carried out, leading to a proposed criterion for incipient separation.

SYMBOLS

c_f	skin-friction coefficient
K	local wall curvature, nondimensional with L^{-1}
L	length of boundary layer, up to shock wave
M_e	Mach number in external flow ahead of shock
P, P_e, P_o	local static pressure, and external-flow static and stagnation pressures ahead of shock, nondimensional with sonic pressure ahead of shock
Re, Re^*	Reynolds number based on L and on external-flow quantities or sonic values
U, U_e	local velocity and external-flow velocity, nondimensional with critical sound speed
u_τ	nondimensional friction velocity; $u_\tau^2 = \frac{1}{2} U_e^2 c_f$
X, x	$\bar{X}/L, (M_e^2 - 1)^{-1/2} x/\delta$; \bar{X} = coordinate along wall
Y, y, \hat{y}	$\bar{Y}/L, Y/\delta, (M_e^2 - 1)^{-1/2} y/u_\tau$; \bar{Y} = coordinate normal to wall
γ	ratio of specific heats
δ	boundary-layer thickness ahead of shock, nondimensional with L
ϵ	$U_e - 1$
κ	von Kármán constant, taken equal to 0.41
Π	pressure-gradient parameter in velocity profile
τ_w	wall shear stress, nondimensional with undisturbed value

PRESSURE DISTRIBUTION

In the velocity defect layer, $y = Y/\delta = O(1)$, where $\delta = O(u_T)$, and ahead of the shock wave $U \sim 1 + \epsilon + u_T u_{01}(y)$, as in figure 1. We take $u_{01} = \kappa^{-1} \ln y - \kappa^{-1} \Pi (1 + \cos \pi y)$ for $0 < y_T < 1$ and $u_{01} = 0$ for $y > 1$ (e.g., ref. 7), where $\kappa = 0.41$ and for zero pressure gradient Π is about 0.5. The sonic line is located at $y = \exp(2\Pi - \kappa\epsilon/u_T)$, and for $u_T \ll \epsilon$ this value is small. In the very thin wall layer $Y = O(u_T^{-1} Re^{-1})$, and the velocity $U = O(u_T)$ has the same form as for an incompressible flow having density and viscosity coefficient equal to the wall values in the actual flow. For $u_T^{-1} Re^{-1} \ll Y \ll \delta$ a mixing-length model is used for the shear stress, and the velocity profile obtained is required to match asymptotically with both the defect-layer and the wall-layer profiles. These matching conditions provide a relationship among the quantities δ , u_T , and Re . A second such relationship is found from the momentum integral equation, in the manner described for incompressible flow, e.g., in reference 7, with quadratic terms in u_T retained. For simplicity the total enthalpy is assumed uniform.

For $Y = O(\delta)$ immediately downstream of the shock wave, the differential equations and shock jump conditions (expanded for $u_T \rightarrow 0$, $\epsilon \rightarrow 0$, and $u_T/\epsilon \rightarrow 0$) show that pressure changes $O(u_T)$ occur over a distance $x = (M_e^2 - 1)^{-1/2} X/\delta = O(1)$. The mean velocity profile has a term $(1 + \epsilon)^{-1}$ plus terms $O(u_T)$ containing a known rotational part and an unknown irrotational part (fig. 2). The shock wave is located at $x = O(u_T/\epsilon)$, and so the shock jump conditions are expanded in Taylor series about $x = 0$. For a first approximation Laplace's equation in the variables x, y is solved in a quarter plane by distributing fluid sources along $x = 0$. For $(x^2 + y^2)^{1/2}$ greater than about 2, it is found that the solution is nearly that due to a point source which represents the change in boundary-layer displacement thickness (as also noted in refs. 3,4). Two correction terms, while formally of higher order, are important numerically at realistic values of u_T and ϵ . One represents changes in vorticity along a streamline of the mean flow; the other accounts for the difference between streamlines and lines $y = \text{constant}$ in the calculation of the rotational part of U , and also enters in the irrotational part through the boundary condition at $x = 0$. The wall pressure with these effects included is

$$P_w/P_e = 1 + 2\gamma\epsilon + \gamma(2\gamma-1)\epsilon^2 + \dots$$

$$+ \{1 + (2\gamma-1)\epsilon\} \frac{4\gamma}{\pi} u_T \left\{ 1 + \frac{3\gamma}{2} \frac{u_T}{\kappa} \frac{2 + 3.18\Pi + 1.5\Pi^2}{1 + \Pi} \right\} x \int_0^\infty \frac{u_{01}(\eta) d\eta}{x^2 + \eta^2} \quad (1)$$

The solution (1) is logarithmically infinite as $x \rightarrow 0$, as must be expected since the overall pressure change is $O(\epsilon)$ rather than $O(u_T)$. Numerical solution of the nonlinear transonic small-disturbance equations would be required to obtain the correct form in a region near $x = 0$ which is small if $u_T/\epsilon \ll 1$. For a wall with longitudinal curvature, the pressure gradient in the inviscid flow behind a normal shock wave has a logarithmic singularity described by

$$\Delta P = \frac{4\gamma K}{\pi} \left\{ x\delta \ln \delta \sqrt{x^2 + y^2} - y\delta \left(\tan^{-1} \frac{y}{x} - \frac{\pi}{4} \right) \right\} \quad (2)$$

The boundary-layer interaction effect for $x = 0(1)$ is not large enough to change this expression, and so a curvature term can simply be added as a correction to equation (1).

The pressure distributions found by adding equations (1) and (2) are compared in figure 3 with experimental results from reference 8. For $M_e = 1.322$ and $Re = 9.4 \times 10^5$, other parameters are calculated as $\epsilon = .247$, $u_\tau = .050$, $\delta = .0182$, and $c_f = .0032$. The shock-wave position found from the data is the origin for the pressure at 15 mm., where $y \approx 4.1$. The origin for the wall pressure is shifted upstream through $\Delta x = 2.87$, equal to the displacement of the shock wave calculated using the fact that the shock-wave slope is proportional to the y-component of velocity at $x = 0$. In the experiments the wall was a plate having longitudinal curvature which can be inferred from the measured pressures immediately behind the shock wave. The change $\Delta P/P_0$ in a y-distance of 15 mm. was taken as .015, giving $K = .21$. The theoretical curves also include a constant streamwise pressure gradient caused by cross-section area change, estimated from the data as $\Delta P/P_0 = .03$ in a distance of 50 mm. The parameter Π was taken equal to the constant-pressure value $\Pi = 0.5$, which leads to a predicted location of the undisturbed sonic line at $y = .36$. If instead $\Pi = 0.4$, the prediction is $y = .30$, whereas the measured value is $y = .29$; this change in Π would influence the pressures only slightly. The wall pressures are in excellent agreement for x greater than about 3; the region $x < 3$ requiring solution of nonlinear equations is relatively large in this case, because the Reynolds number is not high enough for the upstream sonic line to be really close to the wall. The very beginning of the rise in wall pressure can be expressed by an exponential function with known rate of decay but unknown multiplicative constant, as shown in figure 3 with origin chosen tentatively for good agreement with the data. By comparison with numerical results of ref. 2, it should be possible to estimate this constant. The pressures at 15 mm. from the wall are in good agreement except for small x , where the error probably arises from approximating the shock-wave location by $x = 0$; adding the appropriate second-order term is expected to improve the agreement.

WALL SHEAR

The above description of mean-flow perturbations in terms of disturbances in an inviscid rotational flow does not remain valid as $y \rightarrow 0$. For $y = Y/\delta = 0(u_\tau \epsilon^{1/2})$, it is easily found that turbulent stresses as well as pressure and inertia terms must be retained in the boundary-layer momentum equation. This thinner layer (still much thicker than the viscous wall layer) has been called a Reynolds stress sublayer in reference 1 and a blending layer in reference 2. Double expansions as $u_\tau \rightarrow 0$ and $\epsilon \rightarrow 0$ are assumed for the velocity components, pressure, and Reynolds stress, with the latter represented by a simple mixing-length model, chosen for analytical convenience in the belief that the results may not depend strongly on the model used. The wall shear stress has the form

$$\tau_w(x) = 1 + a\epsilon + \frac{1}{2}a(a-1)\epsilon^2 + \dots + u_\tau \tau_{11}(x) + \epsilon u_\tau \{ (\ln \epsilon^{1/2} u_\tau) \tau_{1l}(x) + \tau_{11}(x) \} + \dots \quad (3)$$

where $a = \text{constant}$. This expansion, like that for the pressure, requires modification when x is small. The y-component of velocity and the related displacement

effect of this sublayer are small enough that the previous calculation of pressure is unaffected, and the boundary condition $v = 0$ at $y = 0$ used for $y = 0(1)$ is thereby verified. With use of the solution for pressure evaluated as $y \rightarrow 0$, it is found that $\tau_{11}(x)$ is proportional to the pressure perturbation, and therefore decreases monotonically with increasing x ; also τ_{12} is constant. The term $\tau_{11}(x)$ is obtained as a lengthy expression including terms proportional to the pressure perturbation and a positive term proportional to $\ln x$ (ref. 9). Since the pressure perturbation decreases to zero as x increases (i.e., is small for $\epsilon l/2\delta \ll X \ll 1$), it follows that τ_w has a minimum. Thus for typical values of M_e and Re figure 4 shows that τ_w first decreases sharply and then rises again slowly. At a given x , τ_w decreases as ϵ increases and increases as Re increases. This behavior is in general agreement with existing experimental results.

If it is assumed that equation (3) remains a good approximation even when changes in τ_w are not small as originally assumed, a criterion for incipient separation can be proposed. For example, curve III in figure 4 is drawn for $Re^* = 10^6$ and $M_e = 1.149$, corresponding to $\epsilon = 0.12$; if ϵ is increased to 0.2, the minimum value of τ_w decreases to zero, and this is taken as an indication of incipient separation. Values of M_e corresponding to this condition, namely that $\tau_w = 0$ and $d\tau_w/dx = 0$ simultaneously, are plotted against Re^* in figure 5, and show a slow increase in the shock strength required for separation as Re increases. As a first step toward studying flows with separation, a numerical solution was also carried out for a momentum equation appropriate for describing a slender low-speed separation bubble having length $\Delta x = 0(1)$. Terms were retained to represent the laminar and turbulent stresses and the pressure gradient, which was considered known from the previous solutions because the displacement effect of the bubble was sufficiently small. Velocity profiles obtained are plotted against \hat{y} in figure 6.

CONCLUDING REMARKS

The favorable comparison with experiment shown in the figures for the latter part of the pressure rise seems to imply that the asymptotic representation given here, with the addition of second-order terms as noted, does correctly include the most important features of the local flow field. A study of other second-order terms is continuing, and an analytical solution has been derived for the correction necessary in the flow behind a shock wave in a circular pipe; a comparison with existing experimental results is being carried out. It is anticipated that a comparison with numerical results of Melnick and Grossman will suggest a simple curve fit, in terms of a coordinate nondimensional with the distance to the sonic line, to fill in the wall pressure in the region near the origin. It should now be possible to incorporate these analytical representations for the local pressure and velocity into potential-flow calculations of the transonic flow past an airfoil. The predictions for wall shear, and for the Mach number at which separation first occurs, show the expected trends, and should be checked for quantitative accuracy against existing experimental data. It would seem especially important to continue the attempt at developing a rational theory of separation for turbulent boundary layers.

REFERENCES

1. Adamson, T.C., Jr.; and Feo, A.: Interaction between a Shock Wave and a Turbulent Boundary Layer in Transonic Flow. SIAM J. Appl. Math., vol. 29, 1975, pp. 121-145.
2. Melnik, P.E.; and Grossman, B.: Analysis of the Interaction of a Weak Normal Shock Wave with a Turbulent Boundary Layer. AIAA Paper No. 74-598, 1974.
3. Melnik, R.E.; and Grossman, B.: Further Developments in an Analysis of the Interaction of a Weak Normal Shock Wave with a Turbulent Boundary Layer. Symposium Transsonicum II, K. Oswatitsch and D. Rues, eds. Springer-Verlag, 1976, pp. 262-272.
4. Melnik, R.E.; and Grossman, B.: Interactions of Normal Shock Waves with Turbulent Boundary Layers at Transonic Speeds. Transonic Flow Problems in Turbomachinery, T.C. Adamson, Jr., and M.J. Platzer, eds. Plenum Press, 1977, pp. 415-433.
5. Adamson, T.C., Jr.; and Messiter, A.F.: Normal Shock Wave - Turbulent Boundary Layer Interactions in Transonic Flow near Separation. Transonic Flow Problems in Turbomachinery, T.C. Adamson, Jr., and M.F. Platzer, eds. Plenum Press, 1977, pp. 392-414.
6. Adamson, T.C., Jr.: The Structure of Shock Wave - Turbulent Boundary Layer Interactions in Transonic Flow. Symposium Transsonicum II, K. Oswatitsch and D. Rues, eds. Springer-Verlag, 1976, pp. 244-251.
7. Cebeci, T.; and Smith, A.M.O.: Analysis of Turbulent Boundary Layers. Academic Press, 1974.
8. Ackeret, J.; Feldmann, F.; and Rott, N.: Untersuchungen an Verdichtungsstößen und Grenzschichten in schnell bewegten Gasen. Mitteilungen aus dem Institut für Aerodynamik, ETH Zürich, Nr. 10, 1946. Translated as NACA TM 1113, 1947.
9. Liou, M.S.: Asymptotic Analysis of Interaction between a Normal Shock Wave and a Turbulent Boundary Layer in Transonic Flow. Ph.D. Thesis, Department of Aerospace Engineering, The University of Michigan, 1977.

C-4

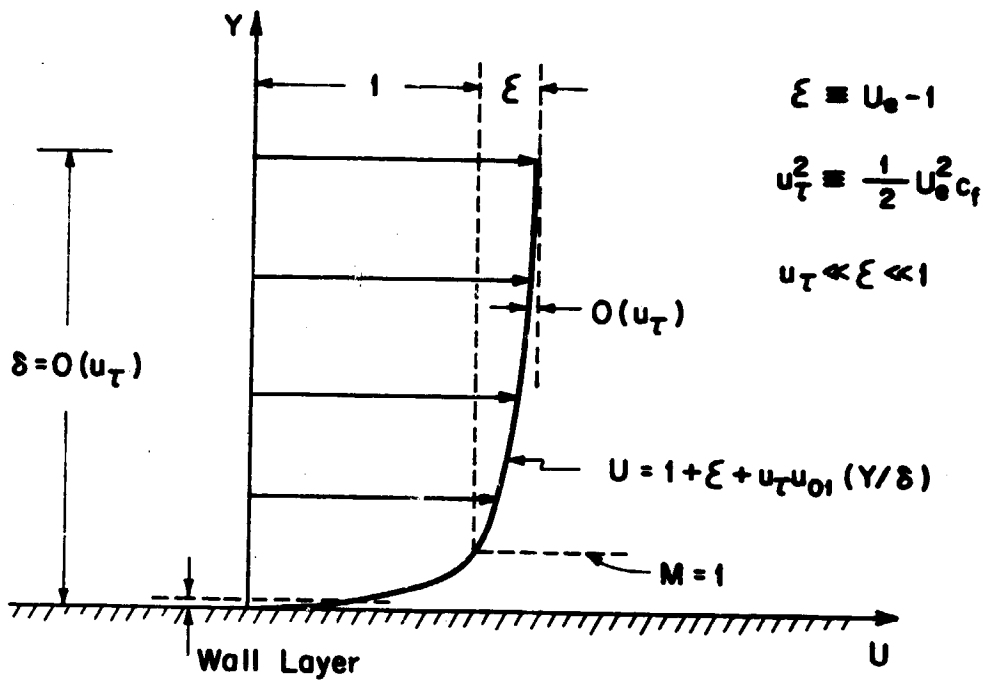


Figure 1.- Velocity profile in undisturbed boundary layer.

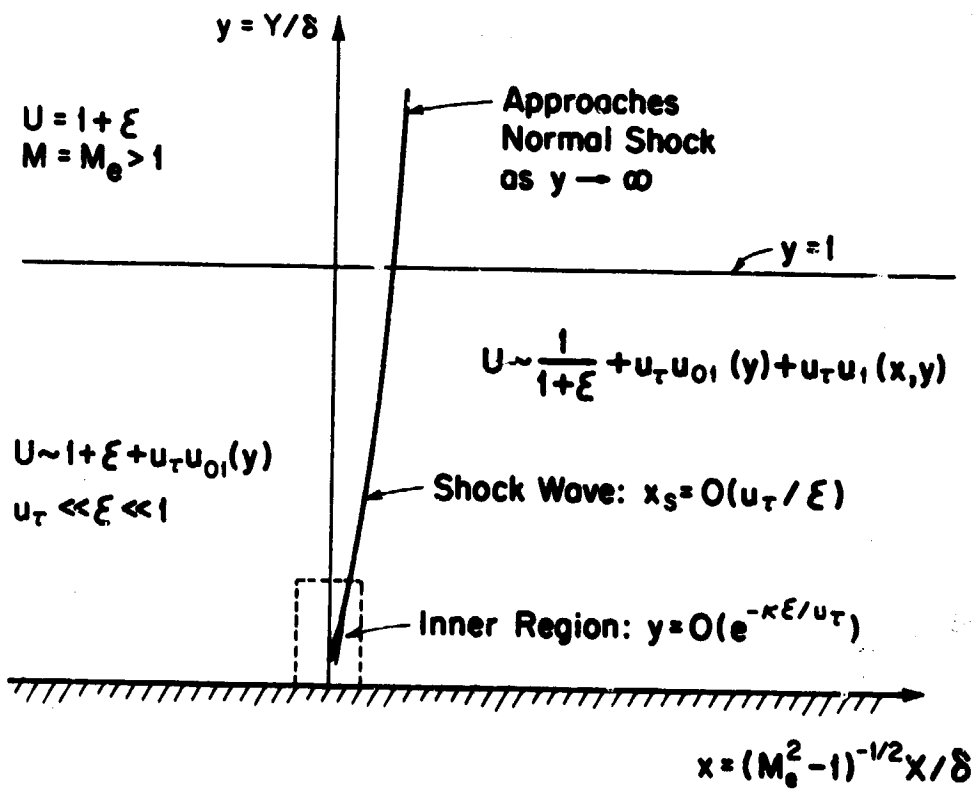


Figure 2.- Representation of outer flow field.

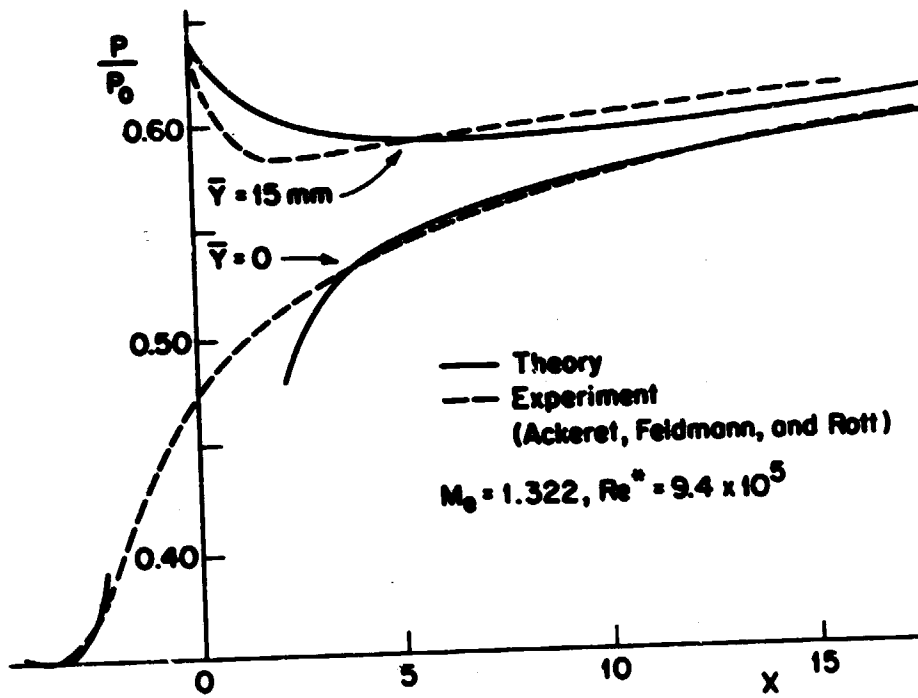


Figure 3.- Pressure distributions.

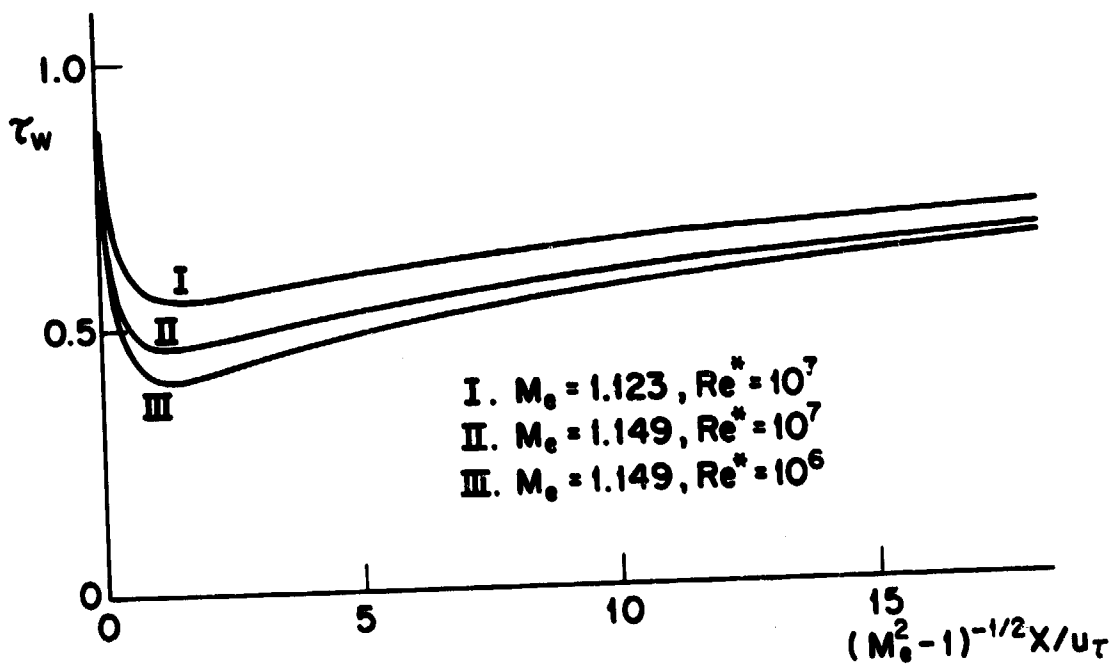


Figure 4.- Predicted wall shear stress.

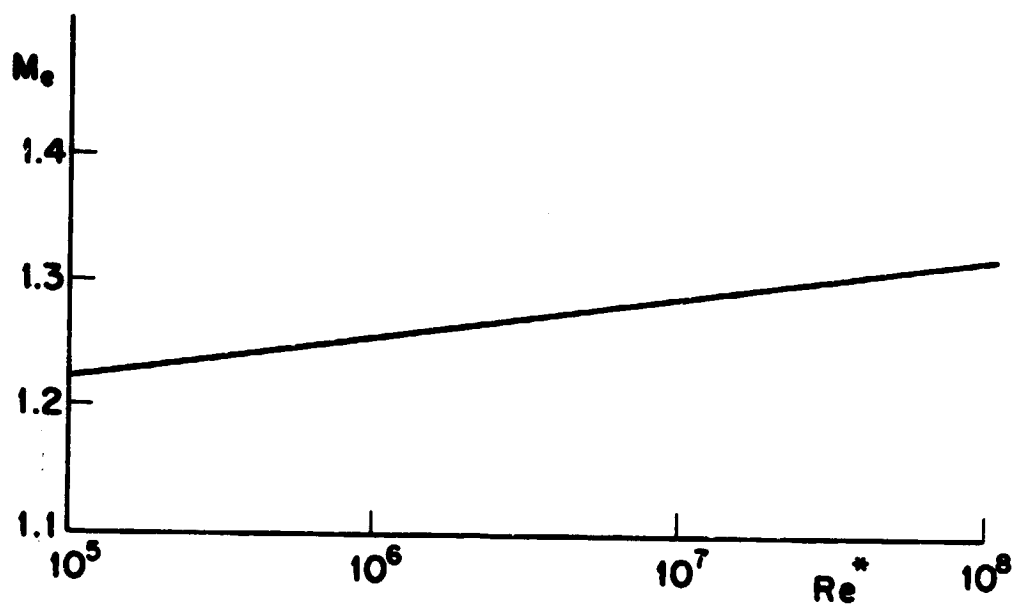


Figure 5.- Predicted variation of Mach number with Reynolds number at incipient separation.

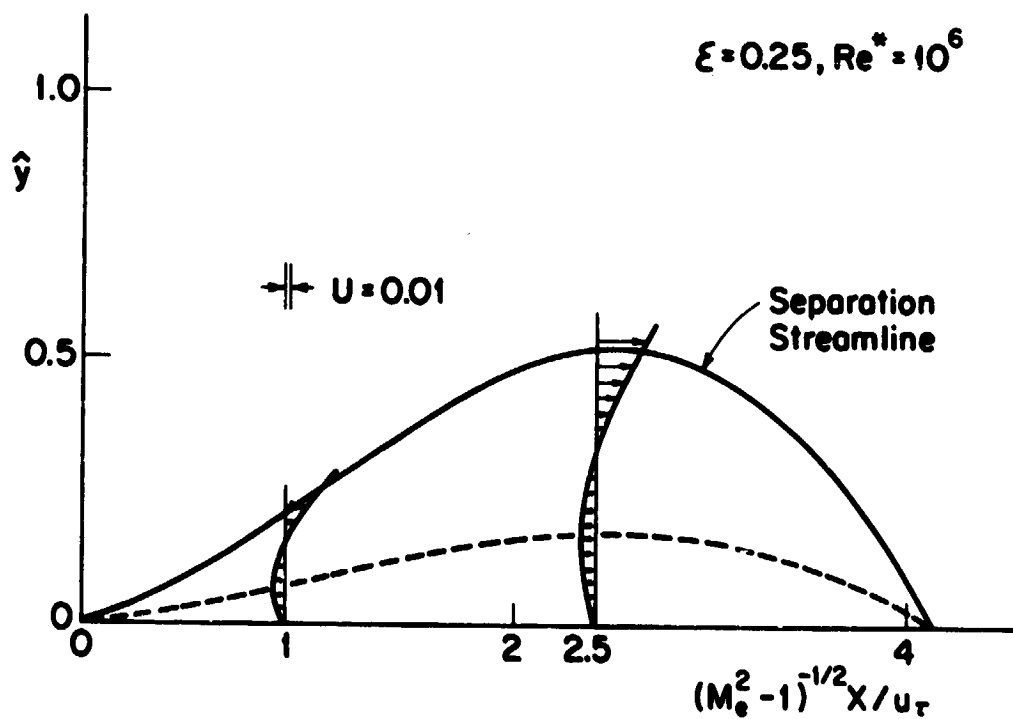


Figure 6.- Calculated velocity profiles in a slender separated-flow region.